Received: 22 December 2024 | Revised: 1 May 2025 | Accepted: 5 May 2025

DOI: 10.1111/vsu.14286

CLINICAL RESEARCH

WILEY

Analysis of humeral condylar morphology in dogs with and without humeral intracondylar fissure

Emily Frapwell MA, VetMB[1] | **Moira Watkins BVMS**[2] | **Bryony Halcrow PhD, MEng, ACGI**[3] | **Heather Goodrum BA Hons, MSc**[3] | **Neil J. Burton BVSc, MResCVR, DSAS (Orth), CertSAS, PGCertHE, FHEA**[1] | **Daniel M. Ogden BVSc, DACVS (Small Animal)**[4] | **Steve Bright BVMS, CertSAS, DipECVS**[5] | **Bill Oxley MA, VetMB, DSAS (Orth)**[3]

[1]Wear Referrals, Part of Linnaeus Veterinary Ltd, Stockton-on-Tees, UK

[2]Queen's Veterinary Hospital, University of Cambridge, Cambridge, UK

[3]Vet3D Ltd, Kendal, UK

[4]Bristol Vet Specialists, Bristol, UK

[5]Manchester Veterinary Specialists, Manchester, UK

Correspondence
Emily Frapwell, Wear Referrals, Bradbury, Stockton-on-Tees, TS21 2ES, UK.
Email: emily.frapwell@wear-referrals.co.uk

Abstract

Objective: To quantify the morphology of the humeral condyle in dogs with and without humeral intracondylar fissure (HIF).

Study design: Retrospective case control.

Sample population: A total of 171 elbows.

Methods: Computed tomography (CT) scans of elbows were retrospectively analyzed. The population comprised three groups; non-chondrodystrophic control dogs ($n = 44$), Springer Spaniel control dogs ($n = 27$), and humeral intracondylar fissure (HIF)-affected dogs ($n = 100$). A condylar template was constructed on three-dimensional (3D) surface-rendered images with measurement of 10 parameters by three observers.

Results: A total of 171 elbows were analyzed. Angle A, representing the axial surface of the medial humeral condyle and angle B, representing the axial surface of the lateral humeral condyle were both significantly greater in HIF-affected dogs ($p < .001$). Length a ($p = .007$) and b ($p < .001$), representing the vertical distance between the most proximal and most distal points of the medial and lateral humeral condyles respectively, were also significantly greater in HIF-affected dogs.

Conclusion: From the population sampled, HIF-affected dogs had both significantly greater vertical height as well as angulation of the axial surface of both the medial and lateral humeral condyle.

Clinical significance: Greater angulation of the axial surfaces of the humeral condylar articular surface could create an intracondylar shear force orthogonal to the orientation of the fissure, predisposing to HIF formation.

The results of this report were presented in abstract form at the Autumn meeting of the British Veterinary Orthopedic Association, November 21–23, 2024.

1 | INTRODUCTION

Humeral intracondylar fissure (HIF) is a common orthopedic condition reported most frequently in spaniel breeds in the UK.[1,2] HIF is characterized by a midsagittal fissure in the humeral condyle,[3] and may extend partially or completely through the isthmus.[4] HIF can be an incidental finding,[5] may be a cause of variable forelimb lameness localized to the elbow[1] or may result in spontaneous elbow fracture.[4]

The etiology of HIF remains uncertain. Historically referred to as incomplete ossification of the humeral condyle (IOHC), it was hypothesized that the defect formed due to a failure of union of the two condylar ossification centers.[2] HIF has been documented in elbows previously confirmed to be normal on both computed tomography (CT)[6,7] and magnetic resonance imaging (MRI),[8] supporting an alternative theory of normal ossification of the condyle with subsequent stress fracture (most probably fatigue fracture due to cyclic application of load that exceeds the capacity of normal bone over time).[9–11] This hypothesis is supported by histopathology findings of fibrous tissue and osteoclastic activity without cartilage in the central zone, and adjacent osteosclerosis,[12,13] the latter feature being associated with the increased radiopacity commonly observed with stress fractures and HIF.[14]

It is possible that both IOHC and HIF are different manifestations of the same disease. It has been suggested that both etiopathogeneses are associated with separate dog populations with IOHC applying to skeletally immature dogs, and HIF in skeletally mature dogs due to stress fracture.[3]

Subsequent to the theory of HIF being due to stress fracture, interest has grown in the possibility that elbow conformation may predispose to HIF formation.[9] It is intuitive that the morphology of the elbow joint, and load interactions between the humerus, radius and ulna, could influence the forces applied through both the trochlear and capitulum of the humeral condyle.

Forces acting upon the condyle have been evaluated in a study investigating failure of transcondylar screws in dogs with IOHC.[15] The authors document implant fracture due to fatigue failure, secondary to multidirectional forces acting upon the screw at the site of the fissure.[16]

Incongruency of the elbow joint has been identified in a proportion of dogs with HIF both on CT[16] and arthroscopic assessment of the joint.[9] Recently, proximal ulnar osteotomy has been shown to have a disease modifying effect on HIF with spontaneous resolution of the fissure in a proportion of dogs following this surgery.[17]

It was the authors' observation that HIF-affected condyles appeared to have a steeper angle of the axial medial portion of the articular surface than unaffected condyles (Figure 1). It was hypothesized this could create an aberrant shear force between the medial and lateral aspects of the condyle, contributing to a mechanism for stress-fracture and thus HIF formation.

The hypothesis for this study was that dogs with HIF have different condylar morphology to dogs not affected by HIF.

2 | MATERIALS AND METHODS

This was a retrospective cohort study comprising client-owned dogs having undergone CT scan of one or both elbows. Ethical approval for this study was gained from the ethics review boards of both CVS UK Group and the University of Cambridge, UK.

2.1 | Data collection

The population comprised client owned dogs which underwent CT scan between 2013 and 2023.

2.1.1 | Control cohort

Groups 1 and 2 were designated as control groups. CT scans were obtained in each case from one of two multidisciplinary referral hospitals (Queen's Veterinary Hospital, University of Cambridge, UK, and Bristol Vet Specialists, Bristol, UK) or Vet3D, UK. Of the dogs presented to either referral hospital, cases for inclusion were identified via a database search by a single researcher (MW). Inclusion criteria were for dogs having undergone CT scan that had included the elbows for reasons unrelated to HIF (e.g., thoracic CT) and whose condyles showed no evidence of HIF. Where the scan included both elbows, only one elbow per dog was used for analysis.

Scans were anonymized and assigned a study number to ensure client confidentiality prior to analysis. Breed and age were recorded.

Control group 1 inclusion criteria were non-chondrodystrophic breeds of dog typically unaffected by HIF.

Control group 2 inclusion criteria were Springer Spaniels over the age of 8.5 years unaffected by HIF. This age criterion was used as 95% Springer Spaniels in group 3 were younger than 8.5 years of age.

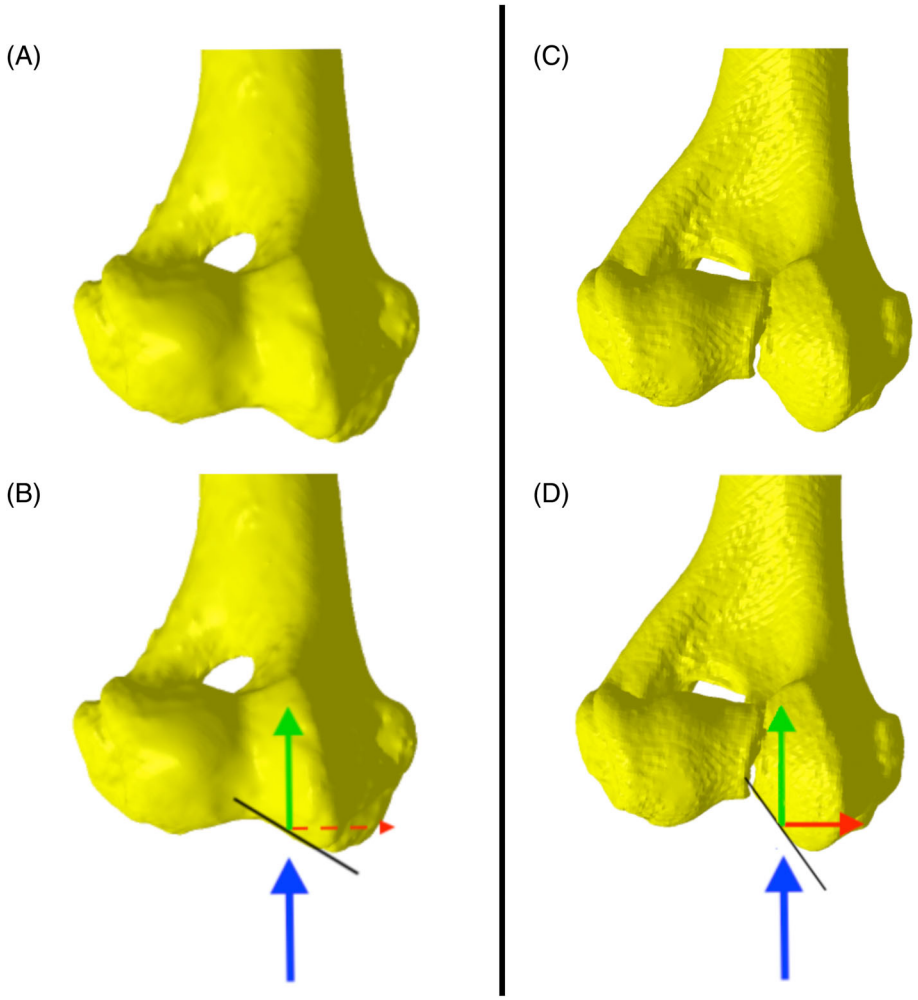

FIGURE 1 A three-dimensional (3D)-rendered model of a distal humerus demonstrating the proposed effect of axial compression on an increased angulation of the medial humeral condyle.

2.1.2 | HIF cohort

Group 3 comprised dogs with HIF on CT. Signalment and lateralization were recorded. CT scans for group 3 were subsequently subdivided into three subgroups;

- HIF1 comprised non-spaniel breeds (and crosses) affected by HIF.
- HIF2 comprised all spaniel breeds (and crosses) affected by HIF.
- HIF3 comprised only Springer Spaniels affected by HIF.

HIF3 group was formulated to permit comparison between solely Springer Spaniels unaffected by HIF (control group 2) and Springer Spaniels affected by HIF.

2.2 | CT analysis

The CT DICOMs were imported into a medical image viewing software (Osirix, Pixmeo, SARL; Geneva, Switzerland). Images were screened for the presence of significant osteophytosis which could have affected the identification landmarks used for condylar morphology quantification. Bone algorithm sequences were used to create surface-rendered representations of the humeri created using standard bone-segmentation Hounsfield unit thresholds. These were exported as STL files to three-dimensional (3D)-modeling software (Geomagics Freeform, 3D Systems, Rock Hill) allowing 3D virtual models of each condyle to be created. The group 3 condylar models were digitally edited such that the HIF defect was not identifiable (Figure 2). This process was localized to the HIF defect and did not alter any of the landmarks used for condylar morphology assessment. In this way, observers were blinded to the HIF status of each condyle during measurement.

The orientation of all the condylar models were standardized within an orthogonal reference frame. In the frontal plane the medial cortex immediately proximal to the condyle was orientated vertically (Figure 3A). In the sagittal plane the caudal cortex of the medial part of the condyle was orientated vertically. In the dorsal plane

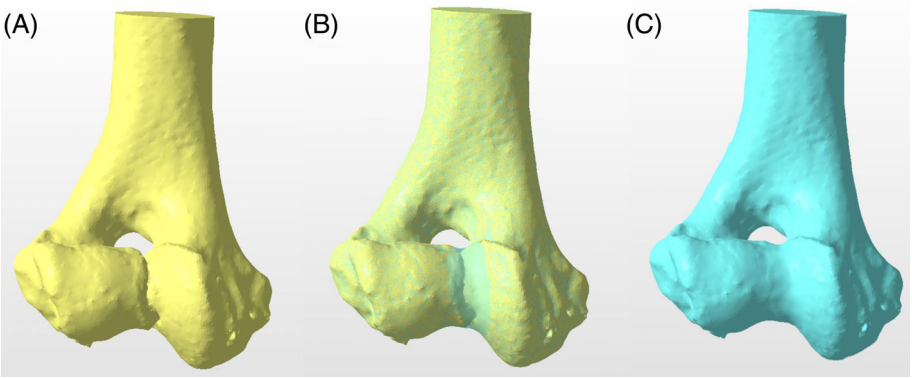

FIGURE 2 (A) Craniocaudal projection of a distal humerus from group 3, with a clearly visible humeral intracondylar fissure (HIF) defect. (B) The defect is rendered to be indistinguishable from a non-HIF elbow using the same color and texture as surrounding bone. (C) The same region following completion of rendering of the intracondylar region.

the abaxial portion of the capitulum was orientated horizontally. Condylar orientation was iteratively adjusted until these criteria were simultaneously satisfied in all three planes.

2.3 | Condylar templating

Following standardization, condylar orientation distance and angular measurements of each condyle were made within the 3D-modeling software. For distance measurements, virtual two-dimensional (2D) planes were superimposed on the 3D model. For frontal plane measurements this plane was orientated in the sagittal plane, and for dorsal plane measurements the plane was orientated in the frontal plane (the virtual plane had no width; the lines in Figure 3B A and B are a schematic representation of the sides of the plane when viewed in each plane). The plane was positioned to intersect the landmarks described in sections 2.3.1 and 2.3.2, and the distance between the planes was determined by the software. For angular measurements a virtual 2D-plane was orientated in the dorsal plane for measurements made in the frontal plane, and in the frontal plane for measurements made in the dorsal plane. The angle between these planes was measured by the software.

2.3.1 | Frontal plane view

Angles A–F, and distances a-f, were measured on a frontal plane view of the condyle as defined in Figure 3A.

- **Angles A–F**: One arm of the angles A–F is a horizonal line drawn parallel to the dorsal plane (red line). The other arm of the angle is drawn to coincide the with the following anatomic landmarks:
  - A – The medial part of the articular surface
  - B – The axial section of the lateral part of the lateral articular surface
  - C – The abaxial section of the lateral part of the lateral articular surface
  - D – A line drawn between the most proximal visible point of the sub-chondral cortex and the most distolateral visible point of the articular surface
  - E – The medial border of the articular surface
  - F – The lateral border of the articular surface
- **Distances a and b:** The vertical distance between the most proximal visible point of the subchondral cortex centrally, to the following anatomic landmarks:
  - a – The most distal visible point medially
  - b – The most distal visible point laterally
- **Distances c–f**: The horizontal distance between the most medial visible point of the medial epicondyle and lines drawn vertically from the following anatomic landmarks:
  - c – The most distal visible point of the subchondral cortex medially
  - d – The most proximal visible point of the subchondral cortex centrally
  - e – The most distal visible point of the subchondral cortex laterally
  - f – The most lateral visible point of the lateral epicondyle

2.3.2 | Dorsal plane view

Angles G, H and I, and distances g and h, were measured on a dorsal plane view of the condyle as defined in Figure 3A.

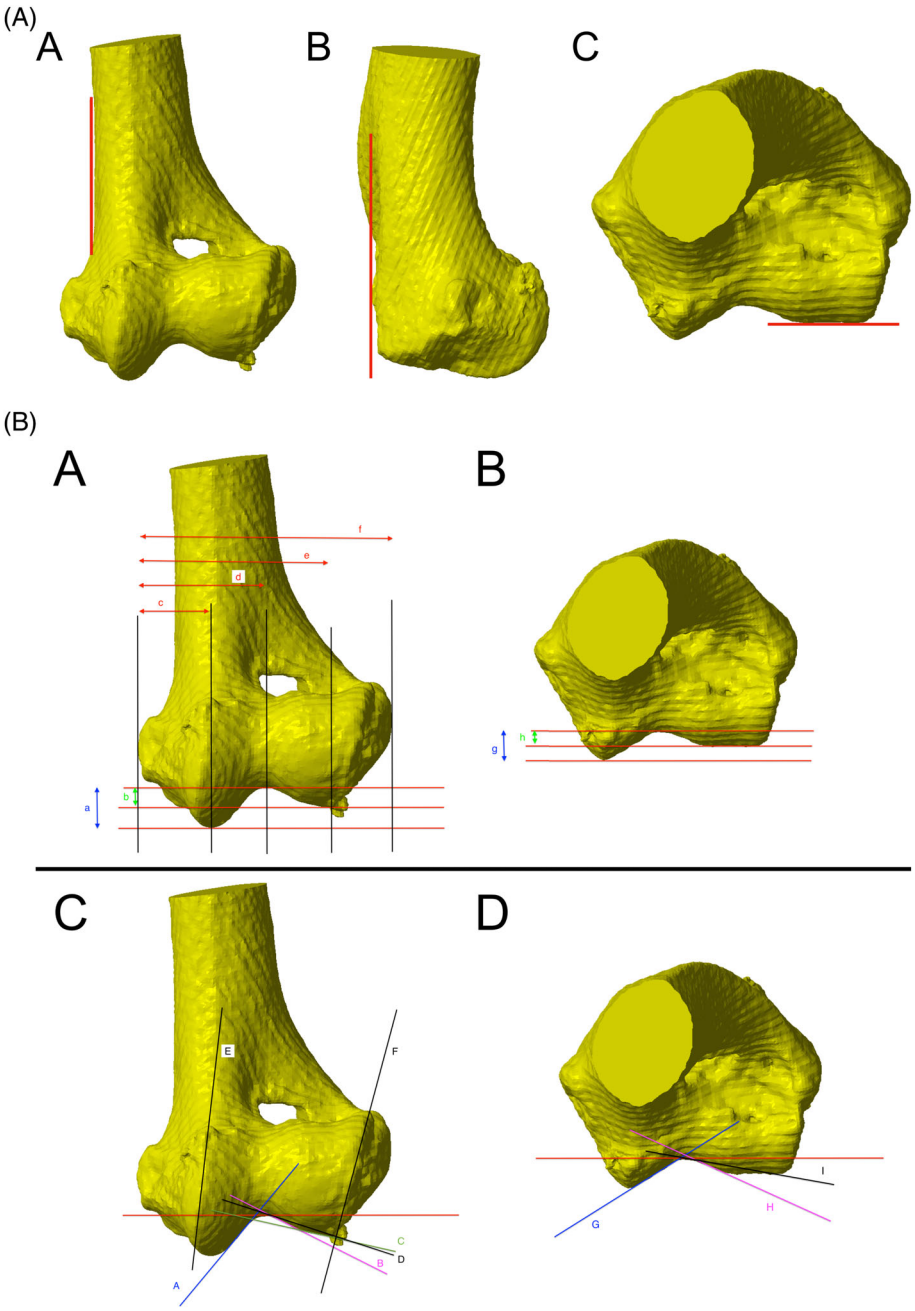

FIGURE 3 (A) A Three-dimensional (3D)-rendered model of a distal humerus, demonstrating orientation in the frontal, sagittal and dorsal planes. (B) 3D-rendered model of a distal humerus, demonstrating distance and angular measurements as listed in sections 2.3.1 and 2.3.2.

- **Angles G, H and I**: One arm of the angles G, H and I is a horizonal line drawn parallel to the frontal plane (red line). The other arm of the angle is drawn to coincide the with the following anatomic landmarks:
  - G – The medial part of the articular surface
  - H – The axial section of the lateral part of the lateral articular surface
  - I – A line drawn between the most caudal visible point of the subchondral cortex and the most craniolateral visible point of the articular surface
- **Distances g and h**: The vertical distance between the most caudal visible point of the subchondral cortex centrally, to the following anatomic landmarks:
  - g – The most cranial visible point medially
  - h – The most cranial visible point laterally

2.4 | Inter-/intraobserver agreement

A pilot study of 20 condyles was initially undertaken to confirm acceptable inter- and intraobserver agreement of the distance and angular measurements described in section 2.3.1, 2.3.2 and Figure 3B. These condyles were selected from the total pool of 171 condyles in the study using a random number generator (www.random.org). All measurements for each of the 20 condyles were performed three times on separate days by three observers (MW, BH, HG). Intra- and interobserver agreement were

assessed with the intraclass correlation coefficient (ICC). Parameters which did not have good or excellent agreement (>0.75)[18] for both inter- and intraobserver correlation were subsequently excluded from the study.

2.5 | Statistical analysis

A total of 100 cases in group 3 were collected and analyzed for the purposes of power calculations, which were performed prior to control group data collection. In comparison to this group of 100 dogs, sample sizes for the control group at a power of 0.80 and a significance of 0.05 were estimated as 18 dogs to detect a mean difference of 5° in angle A and 19 dogs to detect a mean difference of 0.5 in distance b.

Data are summarized by median and range. Comparisons of two groups were made using Mann–Whitney tests, adjusted for ties. Statistical significance was taken as $p < .05$. Analysis was carried out in Minitab21 (Minitab LLC, USA). No adjustment was made for multiple tests, and the reader should be aware that some significant results could have arisen by chance alone.

3 | RESULTS

3.1 | Demographics

CT studies of 171 elbows were analyzed. Control group 1 contained 44 dogs with a median age of 12 months (6–150), and median bodyweight of 22 kg (4.3–54). Age data were unavailable for two of these dogs, and bodyweight data were unavailable for eight of these dogs. The most common breeds were crossbreed ($n = 24$) and Husky ($n = 3$). Control group 2 comprised 27 Springer Spaniels with a median age of 118.5 months (108–156). Age data were unavailable for 13 of these dogs. Bodyweight data was unavailable for this group.

For group 3 (HIF-affected), 100 dogs were included. Their median age was 35 months (4–108) and median weight was 18 kg (4.5–50). Age data were unavailable for six dogs, and bodyweight data were unavailable for five dogs. Lateralization was similar between left ($n = 44$) and right ($n = 46$); in addition, 10 dogs had bilateral HIF. The most common breed was Springer Spaniel ($n = 39$), followed by Cocker Spaniel ($n = 23$) and Labrador Retriever ($n = 12$).

Of the Springer Spaniels with HIF ($n = 39$), 17 were right-sided, 16 were left-sided and six were bilateral. Their median age was 25 months (4–108), and median bodyweight was 18 kg (8.8–26.7).

Excluding spaniels and their crosses, 26 dogs with HIF were included. A total of 15 were right sided, nine

TABLE 1 Inter- and intraobserver agreement for the distance and angular measurements.

Measurement	ICC	95% CI
Interobserver correlation (comparison between raters)		
Calculated distances		
a	0.88	0.77–0.95
b	0.98	0.96–0.99
c	0.96	0.91–0.98
d	1.00	0.99–1.00
e	0.99	0.97–0.99
f	1.00	1.00–1.00
g	1.00	1.00–1.00
h	0.99	0.98–1.00
Calculated angles		
A	0.90	0.80–0.95
B	0.89	0.79–0.95
C	0.06	−0.17 to 0.38
D	0.18	−0.08 – 0.49
E	0.62	0.37–0.81
F	0.51	0.25–0.75
G	0.97	0.94–0.99
H	0.96	0.91–0.98
I	0.65	0.41–0.83
Intraobserver correlation (comparison for repeated measures by the same rater)		
Calculated distances		
a	0.98	0.97–0.99
b	0.99	0.98–0.99
c	0.98	0.97–0.99
d	0.99	0.98–0.99
e	0.99	0.99–0.99
f	1.00	1.00–1.00
g	0.71	0.60–0.81
h	0.37	0.21–0.53
Calculated angles		
A	0.91	0.87–0.94
B	0.85	0.78–0.90
C	0.68	0.56–0.78
D	0.58	0.44–0.70
E	0.66	0.54–0.77
F	0.90	0.86–0.94
G	0.94	0.91–0.96
H	0.94	0.91–0.96
I	0.95	0.93–0.97

Abbreviations: CI, confidence interval; ICC, intraclass correlation coefficient.

TABLE 2 Medians (ranges) for the all control and all HIF groups, together with *p*-values from Mann–Whitney tests.

	All control $n = 71$	All HIF $n = 100$	*p*-value
a	4.52 (2.55–7.12)	5.01 (1.54–10.65)	.041
b	1.91 (0.46–3.54)	2.19 (1.49–5.34)	<.001
c	10.19 (5.27–15.27)	9.49 (6.10–15.11)	.009
d	17.50 (9.53–25.51)	16.52 (11.44–29.74)	.150
e	24.31 (13.33–35.85)	23.23 (16.57–37.94)	.593
f	34.39 (20.23–49.91)	33.21 (23.11–54.73)	.107
g	2.66 (1.14–6.06)	3.24 (1.26–6.74)	<.001
h	1.82 (0.16–4.20)	1.79 (0.64–3.55)	.627
Ratio E–C	0.40 (0.29–0.55)	0.42 (0.35–0.55)	<.001
h over g	0.65 (0.06–2.65)	0.55 (0.13–1.88)	.014
b over a	0.40 (0.13–0.67)	0.45 (0.23–1.55)	.002
A	42.00 (12.70–75.40)	45.20 (30.00–62.20)	<.001
A–B angle	114.2 (74.8–144.3)	107.4 (59.9–131.1)	<.001
B	23.00 (4.10–49.16)	28.50 (16.80–68.90)	<.001
G	29.20 (15.60–50.40)	33.55 (19.30–50.40)	<.001
H	20.10 (4.10–41.60)	20.20 (9.10–33.50)	.541

Note: Significant ($p < .05$) differences are indicated by shading.
Abbreviation: HIF, humeral intracondylar fissure.

were left-sided and two were bilateral. Their median age was 34 months (4–105), and median bodyweight was 20 kg (5.4–50). Age and bodyweight data were unavailable for two dogs. The most common breed was Labrador Retriever ($n = 12$), followed by the French Bulldog ($n = 6$) and German Shepherd dog ($n = 3$).

3.2 | Inter-/intraobserver agreement

Distances g and h, and angles C, D, E, F and I (Table 1) were excluded as they did not reach our criteria for inclusion of inter- and intraobserver agreement >0.75.

Distances a–f, and angles A, B, G and H were therefore retained and measured for all 171 condyles in the study.

3.3 | All controls versus all HIF condyles (controls groups 1 and 2 vs. group 3)

The results of analysis are presented in Table 2. Angle A, B, and G differed significantly between control and HIF-affected groups. When collated, control group 1 and 2 condyles ($n = 71$) had a median angle A of 42.0°, whereas all HIF-affected condyles ($n = 100$) had a median angle of 45.2° ($p < .001$). Angle B had a median of 23.0° (control groups) versus 28.5° (HIF group) ($p < .001$). The median value for angle G was 29.2° (control groups) versus 33.6° (HIF group) ($p < .001$).

Length a was significantly ($p = .007$) different between control groups (median 4.52 mm) and HIF-affected dogs (median 5.01 mm). There were also significant differences in length b which was greater in HIF-affected dogs ($p < .001$), length c which was smaller in HIF-affected dogs ($p = .009$), and length g which was greater in HIF-affected dogs ($p < .001$).

3.4 | Springer Spaniel controls versus Springer Spaniels with HIF (control group 2 vs. HIF 3)

Results are presented in Table 3. In our subpopulation of Springer Spaniels, Angle A was greater in HIF-affected condyles (median angle 44.4°) than in unaffected condyles (median 41.2°) ($p = .007$). Angle B was also greater in affected condyles (median 28.0°) than in unaffected condyles (median 23.9°) ($p < .001$). Distance a was greater in HIF-affected condyles (median 5.12 mm) than in unaffected condyles (median 4.03 mm) ($p < .001$).

3.5 | Non-spaniel controls versus non-spaniels with HIF (control group 1 vs. HIF 1)

There was a high proportion of spaniels in our HIF-affected group (group 3). Therefore, to avoid spaniel

	Springer control ($n = 27$)	Springer HIF ($n = 39$)	p-value
a	4.03 (3.21–5.26)	5.12 (3.78–6.38)	<.001
b	1.77 (1.12–3.11)	2.27 (1.49–4.12)	.001
c	9.55 (7.31–10.55)	9.65 (7.82–11.07)	.273
d	15.90 (13.68–19.16)	17.21 (14.67–20.54)	.011
e	22.96 (17.49–27.27)	23.86 (20.70–28.85)	.016
f	32.39 (27.60–39.64)	33.69 (30.05–39.62)	.201
g	2.42 (1.14–3.24)	3.48 (1.94–5.26)	<.001
h	1.81 (0.46–3.24)	1.89 (0.68–2.77)	.969
Ratio E–C	0.40 (0.32–0.47)	0.43 (0.35–0.48)	.003
h over g	0.80 (0.19–2.65)	0.57 (0.14–1.43)	.008
b over a	0.45 (0.27–0.67)	0.46 (0.25–0.80)	.667
A	41.20 (12.70–50.50)	44.40 (36.20–53.70)	.007
A-B angle	113.2 (103.5–144.3)	108.1 (87.5–117.2)	<.001
B	23.90 (12.60–36.10)	28.00 (19.10–40.40)	.006
G	26.10 (15.60–34.30)	33.10 (19.30–42.50)	<.001
H	22.00 (13.50–36.70)	21.50 (9.80–33.00)	.386

Note: Significant ($p < .05$) differences are indicated by shading.
Abbreviation: HIF, humeral intracondylar fissure.

TABLE 3 Medians (ranges) for the Springer Spaniel control and Springer Spaniels with HIF groups, together with p-values from Mann–Whitney tests.

breeds introducing bias, non-spaniel condyles without HIF ($n = 44$) were compared to non-spaniel condyles with HIF ($n = 26$) (Table 4). Results were broadly consistent with other group analyses; angle A was greater in HIF affected condyles (median 48.7°) than unaffected condyles (median 42.3°) ($p < .001$). Angle B was greater in HIF affected condyles (median 27.0°) than control condyles (median 21.6°) ($p < .001$). Distance a was greater in HIF affected condyles (median 5.39 mm) than in unaffected condyles (median 5.07 mm) ($p = .035$).

4 | DISCUSSION

From the population sampled, our results reveal that humeral condyles with HIF have significantly different morphology than normal condyles; we therefore accept our hypothesis.

Of the measurements performed on the humeral condyle images, several significant differences were consistent across all groups. Angles A and G were significantly greater in HIF-affected condyles indicating a steeper angulation (relative to the transcondylar axis) of the axial articular surface of the medial part of the condyle. Additionally, the angulation of the axial articular surface of the lateral part of the condyle was also steeper in HIF-affected condyles. The angle of the wedge-shaped space between these articular surfaces is therefore more acute in HIF-affected than normal condyles (median 107.4° vs. 114.2°). Using fluoroscopic kinematography Rohwedder et al. demonstrated a joint space width <1 mm at both the medial and lateral aspects of the anconeal process in the loaded joint.[19] It is plausible therefore that in HIF-affected condyles the joint space is too narrow to accommodate the anconeal process, a hypothesis consistent with the previously reported arthroscopic lesions at this location.[9] A similar size mismatch could also occur more distally at the primary site of load-transfer between the condyle and the combined articular surfaces of the medial coronoid process (MCP) and radial head.

In this scenario several mechanisms of abnormal load transfer to the condyle are possible. The most intuitive is a simple wedge effect, where the narrowed space between the articular surfaces causes focal medial and lateral contact with wedge-shaped MCP/radial head, and the anconeal process. Since this focused load transfer occurs at an angled surface a potentially large abaxial directed shear force could be generated for a relatively small increase in angulation, although it is also possible that the greater the angle of the articular surface the greater the abaxially directed vector of force that is generated (Figure 1).

However, the forces applied during weight-bearing are complex and this mechanism may be too simplistic. For example, abnormal focal medial and lateral point loading between the anconeal process and the condyle might be expected to produce a linear pattern of cartilage wear, whereas a previous arthroscopic study of HIF-affected spaniels documented relatively discrete cartilage

TABLE 4 Medians (ranges) for the non-spaniel control and non-spaniels with HIF groups, together with *p*-values from Mann–Whitney tests.

	Control 1 ($n = 44$)	HIF1 ($n = 26$)	*p*-value
a	5.07 (2.55–7.12)	5.39 (3.12–10.65)	.035
b	2.02 (0.46–3.54)	2.14 (1.56–5.34)	.020
c	10.64 (5.27–15.27)	10.39 (6.10–15.11)	.693
d	18.84 (9.53–25.51)	18.86 (12.15–29.74)	.794
e	25.37 (13.33–35.85)	27.77 (16.88–37.94)	.236
f	36.75 (20.23–49.91)	37.88 (23.46–54.73)	.500
g	2.94 (1.33–6.06)	3.73 (1.26–6.74)	.013
h	1.85 (0.16–4.20)	2.00 (0.64–3.55)	.359
Ratio E–C	0.40 (0.29–0.55)	0.44 (0.36–0.55)	.002
h over g	0.64 (0.06–1.99)	0.53 (0.13–1.57)	.282
b over a	0.37 (0.13–0.67)	0.39 (0.23–0.99)	.175
A	42.30 (22.30–75.40)	48.65 (30.00–60.70)	<.001
A–B angle	115.3 (74.8–139.0)	105.0 (59.9–131.1)	<.001
B	21.60 (4.10–49.16)	26.95 (16.80–68.90)	.002
G	31.35 (16.90–50.40)	36.45 (20.10–50.40)	.022
H	19.35 (4.10–41.60)	18.95 (9.10–33.50)	.937

Note: Significant ($p < .05$) differences are indicated by shading.
Abbreviation: HIF, humeral intracondylar fissure.

lesions affecting on the medial condylar articular surface at a point corresponding to the position of the anconeal process at a standing angle.[9] This finding may suggest a more complex pattern of abnormal load transfer in affected elbows, with variation throughout the range of motion of the joint and potentially also with medial-versus-lateral load asymmetry.

The correlation between an abnormal condylar articular surface contour and the occurrence of HIF does not of course imply causality. This would ideally require direct quantification of abnormal force transfer, and/or direct demonstration of the postulated incongruity via analysis of ulnar articular surface morphology. It is also important to acknowledge that other hypotheses for abnormal force transfer are plausible, for example abnormal anconeal process morphology, or a specific alteration in antebrachial conformation. However, whilst the exact mechanism remains unclear, there is now fairly strong evidence that some form of abnormal intracondylar shear force is associated with HIF formation. The spontaneous resolution of HIF in a majority of dogs treated with bi-oblique proximal ulna osteotomy[17] suggests that some form of aberrant humeroulnar interaction was initially present, and is consistent with the formation of HIF after previous absence on advanced imaging.[7–9] Additionally, earlier work documented failure modes of transcondylar screws in dogs with IOHC, finding evidence of fatigue failure secondary to multidirectional forces at the fissure.[15] Since placement of a transcondylar screw does not affect the conformation of the humeral condyle or the force applied during weightbearing, a shear force would continue to act upon the screw and may contribute to the reported pattern of failure. This may also support the possibility of abnormal forces created by the morphological differences identified within this study.

One limitation of this study lies in the population of dogs included. The study population comprised a wide range of ages, from four to 156 months. Whilst it is possible that different etiopathogeneses exist in younger dogs and older dogs, the control group of unaffected non-spaniels and the HIF-affected non-spaniels included dogs of similar age ranges (6–150 months and 4–105 months, respectively). The control group of unaffected spaniels were older than their affected counterparts in order to reduce the risk of including dogs who were yet to develop a HIF in the control population. There is no evidence of a change in elbow conformation through the aging process in this breed. Additionally, as HIF is generally seen in older spaniels, it is likely that if the condylar morphology changed to increase the angulation during growth, that the inclusion of young dogs would reduce the average measured differences demonstrated in our results.

Similarly, a range of breeds and bodyweights were included. Again, weight ranges were similar across control (4.3–54 kg) and affected (5.4–50 kg) non-spaniels. Whilst this does represent a somewhat heterogenous population, it serves to confirm that our findings are consistent across a range of dogs, and is not limited to spaniels.

In summary, this study identified significant differences in humeral condylar morphology in dogs with HIF. Key further work to establish the significance of this finding could include quantification of the morphology of the trochlear notch and anconeal process in HIF-affected dogs versus those without. In addition, mathematical modeling to predict the effect of the morphological differences identified here on intracondylar shear force, or to directly map load transfer across the articular surfaces in normal and affected elbows could be pursued. Should variation in humeral condyle shape be a predisposing factor for HIF, this may facilitate development of future screening programs based on analysis of specific variances in condylar morphology.

AUTHOR CONTRIBUTIONS

Frapwell E, MA, VetMB: Contributed to data interpretation and wrote the manuscript. Watkins M, BVMS, Halcrow B, PhD, MEng, ACGI, and Goodrum H, BA Hons, MSc: Contributed to data collection. Burton NJ, BVSc, MResCVR, DSAS (Orth), CertSAS, PGCertHE, FHEA and Oxley B, MA, VetMB, DSAS (Orth): Contributed to revision of the manuscript and formulation of images. Oxley B, MA, VetMB, DSAS (Orth): Conceived the study. Oxley B, MA, VetMB, DSAS (Orth), Bright S, BVMS, CertSAS, DipECVS and Ogden DM, BVSc, DACVS (Small Animal): Designed the study. All authors provided a critical review of the manuscript and endorse the final version. All authors are aware of their respective contributions and have confidence in the integrity of all contributions.

ACKNOWLEDGMENTS

We would like to thank Tim Sparks, GradIS, PGCert, MSc, PhD for his statistical support. Linnaeus Veterinary Limited supported the costs of the Open Access Publication Charges.

CONFLICT OF INTEREST STATEMENT

Research was conducted in the absence of any commercial or financial relationships that could be construed as a potential conflict of interest.

ORCID

Emily Frapwell https://orcid.org/0000-0001-9262-7449

REFERENCES

1. Hattersley R, McKee M, O'Neill T, et al. Postoperative complications after surgical management of incomplete ossification of the humeral condyle in dogs. *Vet Surg*. 2011;40(6):728-733.
2. Moores AP, Agthe P, Schaafsma IA. Prevalence of incomplete ossification of the humeral condyle and other abnormalities of the elbow in English springer spaniels. *Vet Comp Orthop Traumatol*. 2012;25(3):211-216.
3. Moores AP. Humeral intracondylar fissure in dogs. *Vet Clin North Am Small Anim Pract*. 2021;5(2):421-437.
4. Payne DJL, Sparks TH, Smith MAJ, MacDonald NJ. Computed tomography topographical analysis of incomplete humeral intracondylar fissures in English springer spaniel dogs. *Vet Comp Orthop Traumatol*. 2023;37(2):64-73.
5. Moores AP, Moores AL. The natural history of humeral intracondylar fissure: an observational study of 30 dogs. *J Small Anim Pract*. 2017;58(6):337-341.
6. Witte PG, Bush MA, Scott HW. Propagation of a partial incomplete ossification of the humeral condyle in an American cocker spaniel. *J Small Anim Pract*. 2010;51(11):591-593.
7. Farrell M, Trevail T, Marshall W, Yeadon R, Carmichael S. Computed tomographic documentation of the natural progression of humeral intracondylar fissure in a cocker spaniel. *Vet Surg*. 2011;40(8):966-971.
8. Piola V, Posch B, Radke H, Telintelo G, Herrtage ME. Magnetic resonance imaging features of canine incomplete humeral condyle ossification. *Vet Radiol Ultrasound*. 2012;53(5):560-565.
9. Danielski A, Yeadon R. Humero-anconeal elbow incongruity in spaniel breed dogs with humeral intracondylar fissure: arthroscopic findings. *Vet Surg*. 2022;51(1):117-124.
10. Fredericson M, Jennings F, Beaulieu C, Matheson GO. Stress fractures in athletes. *Top Magn Reson Imaging*. 1995;17(5):309-325.
11. Henry GA, Cole R. Chapter 19 - fracture healing and complications in dogs. In: Thrall DE, ed. *Textbook of Veterinary Diagnostic Radiology*. 7th ed. W.B. Saunders; 2018:366-389.
12. Marcellin-Little DJ, DeYoung DJ, Ferris KK, Berry CM. Incomplete ossification of the humeral condyle in spaniels. *Vet Surg*. 1994;23(6):475-487.
13. Gnudi G, Martini FM, Zanichelli S, et al. Incomplete humeral condylar fracture in two English pointer dogs. *Vet Comp Orthop Traumatol*. 2005;18(4):243-245.
14. Davenport A, Clements D, Dancer S. Humeral intracondylar fissures and intracondylar sclerosis are common CT findings in the limb contralateral to a humeral condylar fracture in French bulldogs and spaniel breeds. *Vet Radiol Ultrasound*. 2023;64(4):686-693.
15. Charles EA, Ness MG, Yeadon R. Failure mode of transcondylar screws used for treatment of incomplete ossification of the humeral condyle in 5 dogs. *Vet Surg*. 2009;38(2):185-191.
16. Carrera I, Hammond GJC, Sullivan M. Computed tomographic features of incomplete ossification of the canine humeral condyle. *Vet Surg*. 2008;37(3):226-231.
17. Danielski A, Quinonero Reinaldos I, Solano MA, Fatone G. Influence of oblique proximal ulnar osteotomy on humeral

intracondylar fissures in 35 spaniel breed dogs. *Vet Surg*. 2024; 53(2):287-301. doi:10.1111/vsu.14061

18. Koo TK, Li MY. A guideline of selecting and reporting intraclass correlation coefficients for reliability research. *J Chiropr Med*. 2016;15(2):155-163.
19. Rohwedder T, Rebentrost P, Böttcher P. Three-dimensional joint kinematics in a canine elbow joint with medial coronoid disease before and after bi-oblique dynamic proximal ulnar osteotomy. *VCOT Open*. 2019;02(2):44-49.

How to cite this article: Frapwell E, Watkins M, Halcrow B, et al. Analysis of humeral condylar morphology in dogs with and without humeral intracondylar fissure. *Veterinary Surgery*. 2025;1-11. doi:10.1111/vsu.14286